

# Spectroscopic Ellipsometry and Fluorescence Study of Thermochromism in an Ultrathin Poly(diacetylene) Film: Reversibility and Transition Kinetics

R. W. Carpick,<sup>†,‡</sup> T. M. Mayer,<sup>§</sup> D. Y. Sasaki,<sup>†</sup> and A. R. Burns<sup>\*,†</sup>

*Biomolecular Materials and Interfaces Department, Sandia National Laboratories, Albuquerque, New Mexico 87185-1413, and Chemical Processing Science Department, Sandia National Laboratories, Albuquerque, New Mexico 87185-0601*

*Received December 2, 1999. In Final Form: February 18, 2000*

We have investigated the thermochromic transition of an ultrathin poly(diacetylene) film. The Langmuir film is composed of three layers of polymerized 10,12-pentacosadiynoic acid [ $\text{CH}_3(\text{CH}_2)_{11}\text{C}\equiv\text{CC}\equiv\text{C}(\text{CH}_2)_8\text{COOH}$ ] (poly-PCDA) organized into crystalline domains on a silicon substrate. Spectroscopic ellipsometry and fluorescence intensity measurements are obtained with in situ temperature control. Poly-PCDA films exhibit a reversible thermal transition between the initial blue form and an intermediate "purple" form that exists only at elevated temperature (between 303 and 333 K), followed by an irreversible transition to the red form after annealing above 320 K. We propose that the purple form is thermally distorted blue poly-PCDA and may represent a transitional configuration in the irreversible conversion to red. This hypothesis is supported by the appearance of unique features in the absorption spectra for each form as derived from the ellipsometry measurements. Significant fluorescence emission occurs only with the red form and is reduced at elevated temperatures while the absorption remains unchanged. Reduced emission is likely related to thermal fluctuations of the hydrocarbon side chains. Time-resolved fluorescence measurements of the irreversible transition have been performed. Using a first-order kinetic analysis of these measurements, we deduce an energy barrier of  $17.6 \pm 1.1 \text{ kcal mol}^{-1}$  between the blue and red forms.

## Introduction

Ultrathin organic films, prepared through methods such as Langmuir deposition or self-assembly,<sup>1,2</sup> offer the possibility of tailoring the optical, mechanical, and chemical properties of surfaces at the molecular scale. Such control of surface properties is required to implement micro- and nanoscale sensors, actuators, and computational devices. Materials that change in response to external stimuli are especially important for such applications. Poly(diacetylene)s (PDAs)<sup>3</sup> merit particular interest as these molecules exhibit strong optical absorption and fluorescence emission that change dramatically with various stimuli, namely, UV absorption (*photochromism*),<sup>4–7</sup> heat (*thermochromism*),<sup>8–10</sup> and ap-

plied stress (*mechanochromism*),<sup>7,11–13</sup> changes in chemical environment such as pH,<sup>14,15</sup> and binding of specific chemical or biological targets to functionalized PDA side chains (*affinochromism/biochromism*).<sup>16–18</sup> Chromatic transitions in PDA can even be studied at the nanometer scale, as we have recently observed and controlled mechanochromism by locally applying shear stresses with scanning probe microscope tips.<sup>7</sup> PDA chromatic transitions, along with other properties such as high third-order nonlinear susceptibility,<sup>19</sup> unique photoconduction characteristics,<sup>20</sup> and strong nanometer-scale friction anisotropy,<sup>21</sup> render PDA an extremely interesting material to study with many potential applications.

Optical absorption in PDAs occurs via a  $\pi$ -to- $\pi^*$  absorption within the linear  $\pi$ -conjugated polymer backbone.<sup>3</sup> In general, PDA chromatic transitions involve a significant shift in absorption from low- to high-energy bands of the visible spectrum; thus the PDA appears to transform from a blue to a red color. The mechanism driving these transitions is not understood in detail. It is believed that molecular conformational changes, such as side chain

\* Corresponding author. Tel: 505-844-9642. Fax: 505-844-5470. E-mail: aburns@sandia.gov.

<sup>†</sup> Biomolecular Materials and Interfaces Department, Sandia National Laboratories.

<sup>‡</sup> Current address: Department of Engineering Physics, University of Wisconsin–Madison, 1500 Engineering Dr., Madison, WI 53706-1687.

<sup>§</sup> Chemical Processing Science Department, Sandia National Laboratories.

(1) Ulman, A. *Introduction to Ultrathin Organic Films from Langmuir–Blodgett to Self-Assembly*; Academic Press: New York, 1991.

(2) Schwartz, D. K. *Surf. Sci. Rep.* **1997**, *27*, 245–334.

(3) Bloor, D.; Chance, R. R. *Polydiacetylenes: Synthesis, Structure, and Electronic Properties*; Martinus Nijhoff: Dordrecht, 1985.

(4) Day, D.; Hub, H. H.; Ringsdorf, H. *Isr. J. Chem.* **1979**, *18*, 325–329.

(5) Tieke, B.; Lieser, G.; Wegner, G. *J. Polym. Sci., Part A: Polym. Chem., Ed.* **1979**, *17*, 1631–1644.

(6) Olmsted, J.; Strand, M. *J. Phys. Chem.* **1983**, *87*, 4790–2.

(7) Carpick, R. W.; Sasaki, D. Y.; Burns, A. R. *Langmuir* **2000**, *16*, 1270–1278.

(8) Wenzel, M.; Atkinson, G. H. *J. Am. Chem. Soc.* **1989**, *111*, 6123–6127.

(9) Lio, A.; Reichert, A.; Ahn, D. J.; Nagy, J. O.; Salmeron, M.; Charych, D. H. *Langmuir* **1997**, *13*, 6524–6532.

(10) Chance, R. R.; Baughman, R. H.; Muller, H.; Eckhardt, C. J. *J. of Chem. Phys.* **1977**, *67*, 3616–18.

(11) Muller, H.; Eckhardt, C. J. *Mol. Cryst. Liquid Cryst.* **1978**, *45*, 313–18.

(12) Nallicheri, R. A.; Rubner, M. F. *Macromolecules* **1991**, *24*, 517–525.

(13) Tomioka, Y.; Tanaka, N.; Imazeki, S. *J. Chem. Phys.* **1989**, *91*, 5694–700.

(14) Cheng, Q.; Stevens, R. C. *Langmuir* **1998**, *14*, 1974–1976.

(15) Jonas, U.; Shah, K.; Norvez, S.; Charych, D. H. *J. Am. Chem. Soc.* **1999**, *121*, 4580–4588.

(16) Charych, D. H.; Nagy, J. O.; Spevak, W.; Bednarski, M. D. *Science* **1993**, *261*, 585–588.

(17) Reichert, A.; Nagy, J. O.; Spevak, W.; Charych, D. J. *Am. Chem. Soc.* **1995**, *117*, 829–830.

(18) Charych, D.; Cheng, Q.; Reichert, A.; Kuziemko, G.; Stroh, M.; Nagy, J. O.; Spevak, W.; Stevens, R. C. *Chem. Biol.* **1996**, *3*, 113–120.

(19) Kobayashi, T. *Optoelectron.—Devices Technol.* **1993**, *8*, 309–32.

(20) Hoofman, R. J. O. M.; Siebbeles, L. D. A.; de Haas, M. P.; Hummel, A.; Bloor, D. J. *J. Chem. Phys.* **1998**, *109*, 1885–93.

(21) Carpick, R. W.; Sasaki, D. Y.; Burns, A. R. *Tribol. Lett.* **1999**, *7*, 79–85.

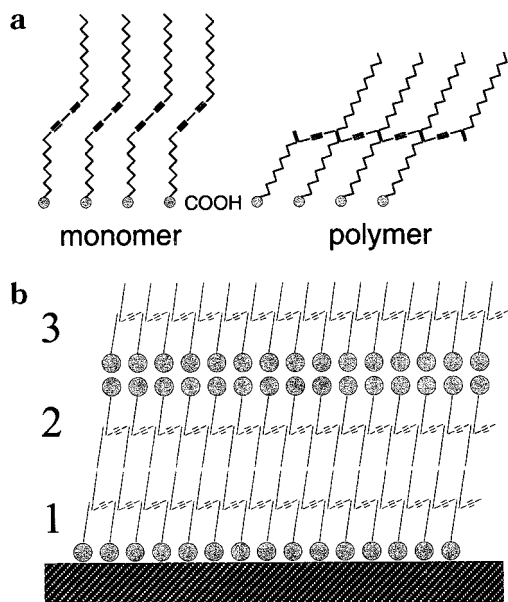


**Figure 1.** (a) Sketch of the monomeric and polymeric form of PCDA molecules. The polymerized form possesses extended linearly conjugated backbones that link the molecules together. The hydrocarbon side chains comprise a large fraction of the molecular structure. (b) Simplified sketch of the trilayer stacking of PCDA molecules. The circles represent the COOH headgroups which are expected to hydrogen bond to the silicon substrate (silicon–layer 1 interface) or with each other (layer 2–layer 3 interface). The polymer backbones (thick lines), which lie parallel to the surface, are aligned in all three layers within a given domain of the film.

packing, ordering, and orientation, impart stresses to the polymer backbone that alter its conformation, thus changing the electronic states and the corresponding optical absorption.<sup>3,9</sup> It is not fully established whether the blue-to-red transitions are continuous transitions or discrete transitions between two or more forms. The factors governing the degree of reversibility of the transitions are also not fully understood.

Our studies of mechanochromism and mechanical properties of ultrathin PDA films<sup>7,21</sup> have prompted us to study thermochromism of the same films to determine the underlying and unifying features of these chromatic transitions. Recent studies of thermochromism in thicker multilayer PDA films have indicated that there is some degree of reversibility to the transition<sup>22–24</sup> involving an intermediate form of the PDA.

The present experiments were conducted using the PDA formed from 10,12-pentacosadiynoic acid [ $\text{CH}_3(\text{CH}_2)_{11}\text{C}\equiv\text{CC}(\text{CH}_2)_8\text{COOH}$ ] (PCDA) monomers ordered on a Langmuir trough (Figure 1a). Our goal was to optimize the film quality. Thus, we avoided the use of metal ion salts in the subphase (e.g.,  $\text{Cd}^{2+}$ ), as we have observed that these generate precipitates on the film.<sup>25</sup> We prepared films consisting of three molecular layers of PCDA, which is the minimum number of layers that can be stabilized on the trough under these conditions.<sup>7,25</sup> Topochemical polymerization was accomplished through UV irradiation of the trilayer on the Langmuir trough.<sup>26</sup> The polymerized PCDA (poly-PCDA) films are then transferred to atomi-

cally flat silicon substrates. Since the opaque substrates preclude performing absorption spectroscopy, we employ spectroscopic ellipsometry and fluorescence intensity measurements to investigate changes upon annealing in the absorption spectrum and fluorescence emission.

## Experimental Section

**Preparation of Trilayer Poly-PCDA Films.** The details of our sample preparation will be described elsewhere.<sup>25</sup> Briefly, both blue and red poly-PCDA films were prepared via UV polymerization on a Langmuir trough (Nima, Coventry, U.K.). The trough was situated on a vibration-isolation table inside a class 100 clean room. The subphase was deionized water with a resistivity greater than  $18\text{ M}\Omega\text{ cm}$  (Barnstead Nanopure system, Dubuque, IA) held at a temperature of  $15 \pm 1\text{ }^\circ\text{C}$ . Si substrates with either native or thermally grown oxide were cleaned in organic solvents followed by a 50/50 mixture of  $\text{H}_2\text{O}_2$  and 30%  $\text{H}_2\text{SO}_4$  for 20 min at  $100\text{ }^\circ\text{C}$  and then immediately rinsed and stored in subphase-quality water before transfer to the Langmuir trough. This rendered the substrates hydrophilic and clean, as high-resolution atomic force microscope (AFM) images obtained in air shortly after rinsing indicated very little observable contamination. From AFM measurements we also verified that the substrates were extremely flat, with  $<0.2\text{ nm}$  root mean square roughness. Just prior to monolayer spreading, the substrates were removed from water storage and completely immersed into the subphase, minimizing exposure to clean room air. The Si substrate was seated horizontally approximately 1 mm below the water surface before spreading the molecules.

PCDA molecules (Farchan/GFS Chemicals, Powell, OH) that had been purified through a silica gel column were spread onto the subphase in a 50% chloroform/benzene solution. On the pure water subphase the monolayer was unstable. However, as the monomer was compressed at a rate of  $100\text{ cm}^2\text{ min}^{-1}$  (molar compression rate  $380\text{ m}^2\text{ s}^{-1}\text{ mol}^{-1}$  or  $4\text{ \AA}^2\text{ molecule}^{-1}\text{ min}^{-1}$ ) to a pressure of  $20\text{ mN m}^{-1}$ , a stable trilayer was produced (molecular area of  $\sim 8\text{ \AA}^2$  for three layers).<sup>25,27</sup> The film possesses the Y-type configuration, which is common for these amphiphilic molecules, as shown in Figure 1b. All films were equilibrated for 20 min at  $20\text{ mN m}^{-1}$ , prior to UV light exposure from a pair of Hg pen lamps (Oriel, Stratford, CT). To produce a blue film, the pen lamps were fixed 10 cm from the water surface and switched on for 30 s. This produced a faintly visible, uniform blue film. Red films were produced by using extended UV exposure. In this case, the pen lamps were fixed at 6 cm from the water surface and switched on for 5 min. This produced a clearly visible red film.

In either case, the water level was then lowered by slowly draining the trough, allowing the polymerized film to drape itself over the substrate. Samples were dried in clean room air and stored in a dark, nitrogen-purged container. A sample that is converted from blue to red by UV irradiation is referred to as a "photochromic" red sample; a sample converted from blue to red thermally is referred to as a "thermochromic" red sample.

**Spectroscopic Ellipsometry Measurements.** A variable angle spectroscopic ellipsometer (J. A. Woollam Co., Lincoln, NE) was employed for ellipsometric studies. Ellipsometry<sup>28</sup> measures the ratio of the complex reflection coefficients,  $r$ , of the p and s polarization components of a beam of polarized light reflected from a surface in terms of two angles,  $\Psi$  and  $\Delta$ , where

$$r^p/r^s = \tan \psi e^{i\Delta} \quad (1)$$

In eq 1,  $\tan \Psi$  and  $\Delta$  are the ratio of the magnitudes and the phase difference between the p and s reflection coefficients, respectively. The reflection coefficients are related to physical characteristics of the sample, such as index of refraction, film thickness, etc., through the Fresnel equations. To extract these sample characteristics, we must construct an optical model of

(22) Mino, N.; Tamura, H.; Ogawa, K. *Langmuir* **1991**, *7*, 2336–2341.

(23) Deckert, A. A.; Fallon, L.; Kiernan, L.; Cashin, C.; Perrone, A.; Encalarte, T. *Langmuir* **1994**, *10*, 1948–1954.

(24) Deckert, A. A.; Horne, J. C.; Valentine, B.; Kiernan, L.; Fallon, L. *Langmuir* **1995**, *11*, 643–649.

(25) Sasaki, D. Y.; Carpick, R. W.; Burns, A. R. Submitted for publication in *J. Colloid Interface Sci.*

(26) Mowery, M. D.; Menzel, H.; Cai, M.; Evans, C. E. *Langmuir* **1998**, *14*, 5594–5602.

(27) Goettgens, B. M.; Tillmann, R. W.; Radmacher, M.; Gaub, H. E. *Langmuir* **1992**, *8*, 1768–1774.

(28) Azzam, R. M. A.; Bashara, N. M. *Ellipsometry and Polarized Light*; North-Holland: Amsterdam, 1987.

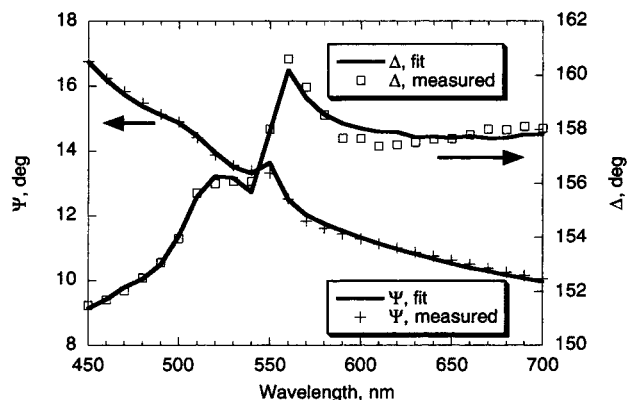


**Figure 2.** Spectroscopic ellipsometric measurement of photochromic red poly-PCDA trilayer film. Angle of incidence is 70°. Fit to the data is obtained using a Lorentz oscillator model for the poly-PCDA complex index of refraction.

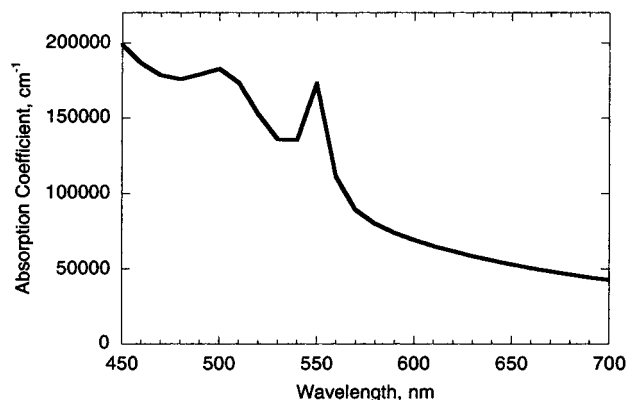


**Figure 3.** Absorption coefficient for photochromic red poly-PCDA film determined from ellipsometric measurements of Figure 2.

the sample, calculate  $\Psi$  and  $\Delta$  for the model, and then fit the model to the experimental results. For the present case of a thin film of poly-PCDA on a Si substrate with a native oxide, we employ a model in which the well-known optical properties of the substrate are used, and the thickness of the film is determined from AFM measurements. We then extract the complex index of refraction of the film as a function of wavelength. The imaginary part of the index (the extinction coefficient,  $k$ ) of the film is related to the absorption coefficient,  $\alpha$ , via

$$\alpha = 4\pi k/\lambda \quad (2)$$

As an example of such a measurement, Figure 2 shows ellipsometric data from a photochromic red poly-PCDA trilayer film at room temperature from 450 to 700 nm, measured at 70° angle of incidence. Also shown in the figure are fits to the data using a Lorentz oscillator parametrization of the complex index of refraction (see Appendix). The absorption coefficient,  $\alpha$ , extracted from this fit (Figure 3) shows a major absorption feature at 550 nm, with a smaller feature at 500 nm. The blue film shows a major absorption feature at 640 nm (Figure 4). These spectra are consistent with previous absorption studies of various PDA films.<sup>9,22–24</sup>

Sample temperature during the measurements is controlled with a small home-built heat/cool stage with an operating range of 270–370 K. A thermoelectric element is attached to the bottom of a copper block (12 × 12 × 4 mm). By use of thermally conductive paste, the sample is attached on top of the copper block to provide uniform sample heating. A solid-state temperature sensor is embedded in the block for temperature readout and regulation using a control unit (Wavelength Electronics, Bozeman, MT). After any change in temperature, the stage was allowed to equilibrate for approximately 1 min before measurement. Once equilibrated, the temperature was stable to within  $\pm 0.5^\circ$ . Ellipsometric measurements are made at fixed temperatures

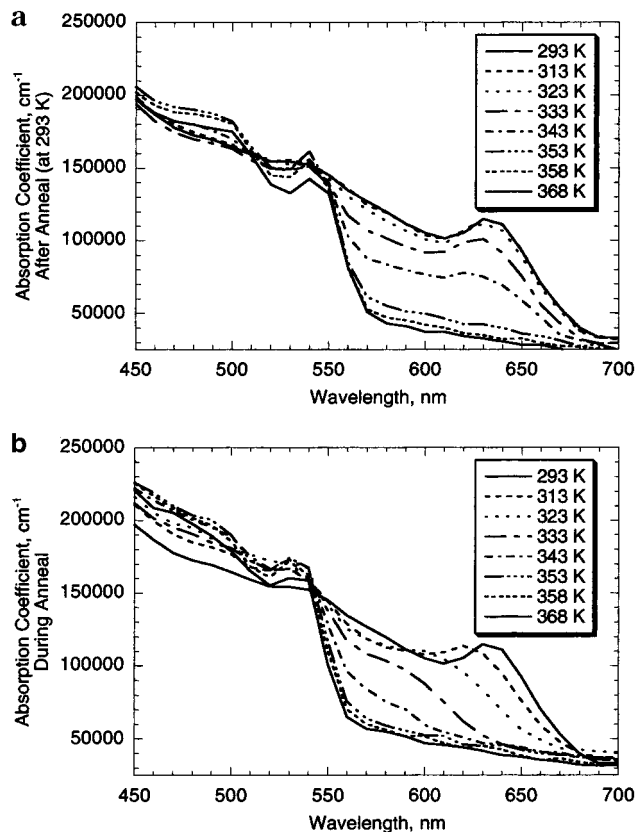


**Figure 4.** (a) Absorption spectra determined from ellipsometric measurements obtained at room temperature, after annealing to the indicated temperatures. The sample is initially a blue poly-PCDA film. Spectra at several temperatures are omitted for clarity. (b) The corresponding absorption spectra obtained while annealing at the indicated temperatures.

over the wavelength range 400–700 nm. A series of annealing and quenching steps were carried out, as described in more detail below. The total time at any given annealing temperature was approximately 2 min.

**Microscopic Fluorescence Intensity Measurements at Fixed Temperatures.** Microscopic sample fluorescence was recorded using a Leitz optical fluorescence microscope equipped with a xenon lamp and dichroic beam filters. The sample was illuminated with 520–550 nm light, and emission wavelengths greater than 590 nm were passed to an intensified CCD camera and digitized. The field of view was  $170 \times 130 \mu\text{m}^2$ . Temperature was controlled with the same heat/cool stage used for the ellipsometry measurements. As with those measurements, the stage was equilibrated for approximately 1 min before measurement after any temperature change, and the total time at any given annealing temperature was approximately 2 min, as with the ellipsometric measurements. Throughout a given series of measurements, the same region of the sample was observed at several different fixed temperatures. Therefore, any observed changes in fluorescence intensity are due to annealing and not to spatial inhomogeneity of the sample. For each measurement, 16 frames were averaged together and the total fluorescence intensity of the image was calculated. This method allows highly accurate, but relatively slow, measurements of fluorescence intensity.

**Time-Resolved Fluorescence Intensity Measurements.** To obtain time-resolved measurements of the thermal transition, an optical platform incorporating a CCD spectrometer with fiber optic collection was set up to measure fluorescence spectra. The temperature was controlled with the same heat/cool stage used for the previous measurements. Poly-PCDA fluorescence was recorded using a fiber-optic-coupled spectrometer (Ocean Optics, Inc., Dunedin, FL), interfaced to a PC using LabView (National Instruments, Austin, TX) data acquisition control. Fluorescence spectra were acquired continuously with a 250 ms integration

time per spectrum. A 550 nm cutoff filter was inserted in the collection path to reduce capturing the excitation light from the blue LED source. Each spectrum was integrated between 585 and 720 nm to completely avoid including any of the remaining excitation light. To carry out the experiment, a background measurement was conducted with the stage at room temperature and a fresh blue sample in place. The sample was then removed, and thermally conducting paste was applied to the stage, which was then allowed to equilibrate at the desired elevated temperature. The underside of the sample was also coated with thermally conducting paste. Data acquisition was then started, and the sample was quickly placed in firm contact with the stage. We calculate that the sample equilibrates with the heater within a few milliseconds, while the conversion from blue to red occurs at an substantially slower rate. Therefore, we assert that the experiment is essentially isothermal. Each measurement is performed on a fresh sample cut from the same substrate. Several measurements are obtained at each temperature over the observable range.

### Initial Film Characterization

The poly-PCDA film quality is nearly identical to films we produced on mica substrates that are described in substantial detail elsewhere.<sup>7,25</sup> To summarize, AFM images confirm that both blue and photochromic red films are organized into uniform, atomically flat crystalline domains up to 100  $\mu\text{m}$  in size. The film covers >90% of the substrate. High-resolution images within the domains reveal large, extended arrays of parallel striations, similar to previous reports.<sup>9</sup> The striations correspond to the backbone direction. This indicates that the backbones are highly oriented within individual domains. Between and within some domains are cracks which expose the substrate, allowing film height measurements that confirm that the film is indeed a trilayer. The photochromic red film is observed to be  $\sim 15\%$  taller than the blue film, which is due to the reduced degree of tilt of the molecules.<sup>7,9,29</sup> In addition, islands are occasionally found on top of the trilayer. AFM height measurements indicate that the islands are an additional bilayer of poly-PCDA. The bilayers are likely stabilized by interfacial hydrogen-bonded ad-dimers of the acid headgroups (as in Figure 1b, between layers 2 and 3). We believe that the bilayers are produced during the monomer compression stage before polymerization and deposition. The bilayer islands cover less than 10% of the underlying trilayer film. Thus, to a good approximation the average film thickness of the trilayer height is  $7.4 \pm 0.8$  nm for the blue film and  $9.0 \pm 0.9$  nm for the photochromic red film.

Strong fluorescence emission is observed from photochromic red films, as well as from thermochromic red films as discussed in the next section. In general, fluorescence emission from PDAs is polarized along the backbone direction.<sup>30–32</sup> Using polarized fluorescence microscopy, we can extinguish the emission from a given trilayer domain by analyzing the emission at  $90^\circ$  to the backbone direction.<sup>7</sup> This confirms that the conjugated backbones within each domain are highly ordered and that there is structural registry between the three layers of both photochromic and thermochromic red films. In other words, the backbones are oriented along the same direction in all three layers within a domain. Thus, the crystallinity of the domains exists not only parallel to the substrate

but also normal to it as well. This is a particular advantage of using a single-transfer film. It is not established, and not likely, that thicker multilayer Langmuir–Blodgett films formed by multiple dips exhibit such structural registry normal to the substrate.<sup>2</sup> This may significantly affect the phase transformation behavior. In addition, these ultrathin films are attractive materials since they can be end-functionalized to provide colorimetric detection of molecules that bind to the functional group.<sup>16–18</sup>

### Results

To investigate the thermochromic transition of the poly-PCDA film, we obtained ellipsometry and fluorescence measurements on a film initially prepared in the blue form. For both sets of measurements, the temperature was varied as follows. The sample was annealed at a fixed temperature, and the measurement (ellipsometric or fluorescence) was acquired at that temperature. The sample was then quenched to 293 K, where a room-temperature measurement was acquired. The sample was then annealed at a temperature 5 deg higher than the previous anneal, and the next measurement was acquired. The sample was then quenched to room-temperature again, and so on. The first anneal temperature was 303 K, and the final anneal temperature was 368 K. In this way we can determine the extent of reversibility after annealing at each temperature and follow the progressive conversion from the blue to red forms of a single region of a given sample.

Shown in Figure 4 are absorption spectra derived from the ellipsometry measurements. Figure 4a shows the *room temperature* absorption after annealing to the indicated temperature. Figure 4b shows the absorption obtained *at* the annealing temperature. Note that the absorption features of the final thermochromic red film are not as pronounced as those for the photochromic red film shown in Figure 3. The room-temperature spectra demonstrate that the major absorption feature of the blue form at 640 nm disappears and the red-form absorption features at 550 and 500 nm appear as the annealing temperature increases. At intermediate annealing temperatures, the 640 nm feature appears to shift to a shorter wavelength, resulting in an apparent new broad absorption feature at 600 nm. This feature is only observed at elevated temperatures (Figure 4b) and is not present in measurements made at room temperature either before or after annealing (Figure 4a). Furthermore it is only observed upon annealing a film originally in the blue form. Material exhibiting this absorption feature we call the “purple” form of the material. Deckert et al.<sup>23,24</sup> have postulated the existence of an intermediate “purple” form based on kinetic aspects of the transition from blue to red.

We would like to know the temperature at which the blue-to-red transition takes place, as well as the relative concentrations of blue and red form that exist at room temperature after each annealing temperature. To do this we assume that the sample consists solely of blue form at the start of the annealing study and solely of the thermochromic red form after annealing to 368 K. Then considering the film to be made up of a mixture of blue and red forms *at room temperature* after each annealing cycle, we construct an effective index of refraction for the film using the Bruggeman effective medium approximation (EMA).<sup>33,34</sup> This procedure is commonly used to

(29) Fischetti, R. F.; Filipkowski, M.; Garito, A. F.; Blasie, J. K. *Phys. Rev. B* **1988**, *37*, 4714–26.

(30) Chance, R. R.; Patel, G. N.; Witt, J. D. *J. Chem. Phys.* **1979**, *71*, 206–11.

(31) Moers, M. H. P.; Gaub, H. E.; Vanhulst, N. F. *Langmuir* **1994**, *10*, 2774–2777.

(32) Yamada, S.; Shimoyama, Y. *Jpn. J. Appl. Phys.* **1996**, *35*, 4480–4485.

(33) Aspnes, D. E.; Theeten, J. B.; Hottier, F. *Phys. Rev. B* **1979**, *20*, 3292.

(34) Tompkins, H. *A Users Guide to Ellipsometry*; Academic Press: San Diego, CA, 1993.

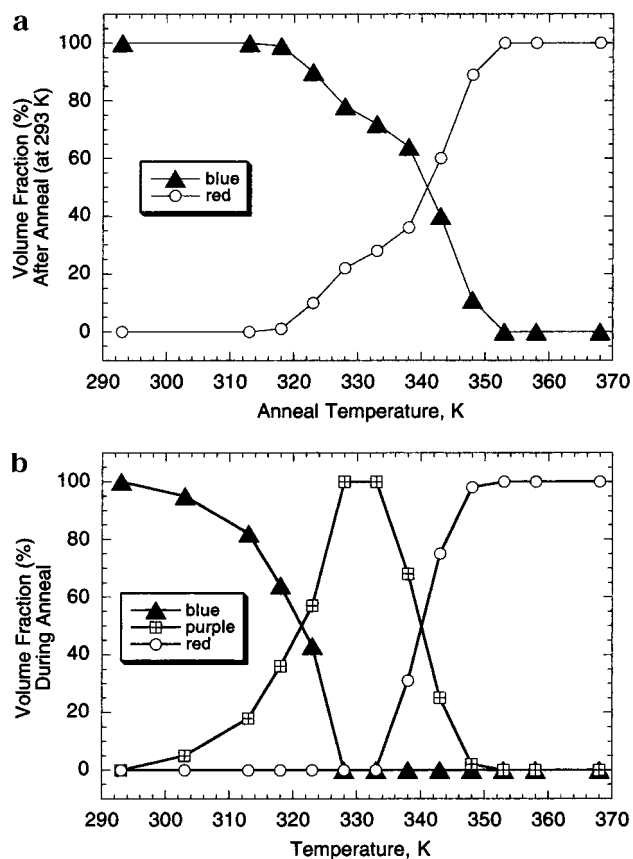


**Figure 5.** (a) Volume fractions of blue and thermochromic red form poly-PCDA in the film at room temperature after annealing to the indicated temperature. (b) “Effective” volume fractions of blue, purple, and red form poly-PCDA in the film at the anneal temperature. It is implicitly assumed that the film entirely consists of the purple form at 333 K; this plot is meant to illustrate the temperature ranges over which each form is created or lost.

analyze multicomponent materials and, when fit to the experimental data, yields the volume fractions of the constituent materials in the film (see Appendix). Applying this two-component model provides good fits to all of the spectra of Figure 4a. The resulting volume fractions are shown in Figure 5a. Starting at about 320 K, a significant fraction of the blue form is converted to red, with near complete conversion after annealing to 353 K. We do not observe any reversion from red back to blue. Annealing a film initially in the red form does not produce any of the blue form.

Absorption spectra derived at each annealing temperature between 320 and 350 K (Figure 4b) indicate the shift of the blue absorption feature to the “purple form”. Assuming this to be a distinct form of the poly-PCDA, and that all blue form has been converted to purple at 328 K (where the purple feature is maximized), we apply a three-component EMA analysis (see Appendix) to the ellipsometric spectra of Figure 4b. This gives the volume fractions of blue, purple, and red forms at the annealing temperatures. The result is shown in Figure 5b. While the assumptions underlying this analysis are not completely rigorous, it allows us to illustrate the temperatures at which each form is created, and the pathways for conversion of the material from blue to red. Examination of Figure 5 shows that the purple form reverts primarily to blue after quenching to room temperature, with approximately 30% converting to red after annealing to 330–340 K and then quenching to room temperature. It is very likely that the ratio of red to blue material formed

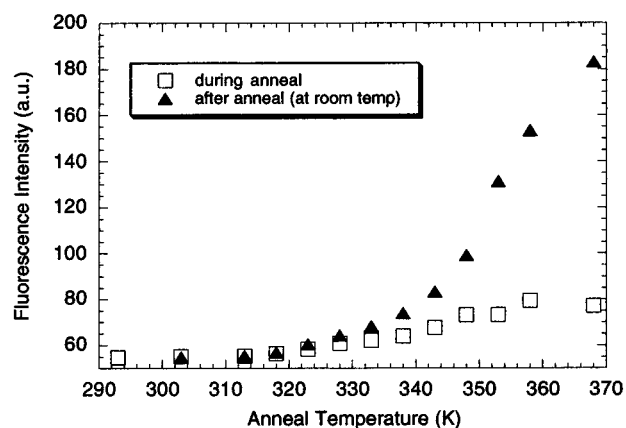


**Figure 6.** Fluorescence emission intensity vs temperature for a sample initially in the blue form: open squares, intensity at the annealing temperature; closed triangles, intensity at room temperature after annealing to the indicated temperature. Substantial emission does not occur until the sample is annealed above 320 K, corresponding to the onset of the formation of red poly-PCDA observed with spectroscopic ellipsometry.

at each annealing increment depends on the length of time the sample was held at the annealing temperature. However, this was not investigated in the present study.

Microscopic fluorescence intensity measurements made on a sample taken from the same film confirm the transition to the red form that is observed in the ellipsometric measurements. Figure 6 displays total fluorescence intensity for an initially blue sample, both during annealing and after quenching to room temperature. Initially, the blue sample displays almost no fluorescence. Fluorescence is also very low at temperatures where the purple form exists (313–343 K). Strong fluorescence begins to appear in the room-temperature measurements after the sample is annealed above 320 K. This coincides with the appearance of the red form in the ellipsometric data of Figure 5a. We have reported the room-temperature fluorescence spectrum elsewhere.<sup>7</sup> It consists of a large peak at 640 nm and a smaller peak at 560 nm. While the ellipsometric absorption data indicate that conversion to the red form was complete above 353 K, the fluorescence emission further increases between the final two experimental annealing cycles at 363 and 368 K. Thus, the fluorescence intensity may be more sensitive to the structure of the film than the absorption. This effect may also partially result from somewhat different heating and cooling rates in the two measurements.

The fluorescence intensity of thermochromic red films is strongly diminished at elevated temperatures. As seen in Figure 6, substantial fluorescence from the red form at room temperature (solid triangles) is reduced when the sample is being annealed (open squares). To completely separate this effect from fluorescence changes occurring due to the blue-to-red transition, we obtained microscopic fluorescence intensity measurements on a photochromic red film using the same series of anneal and quenching steps. Figure 7 shows that fluorescence is also strongly reduced at elevated temperatures for the photochromic red film. Yet, according to the ellipsometric measurements, these films maintain their characteristic red absorption spectrum at elevated temperatures. This effect is reversible, as the fluorescence emission recovers after quenching to room temperature. Furthermore, as seen in Figure 7, cooling the sample below room temperature leads to an increase in fluorescence emission. Thus, fluorescence emission for red films has a completely reversible and distinct temperature dependence.

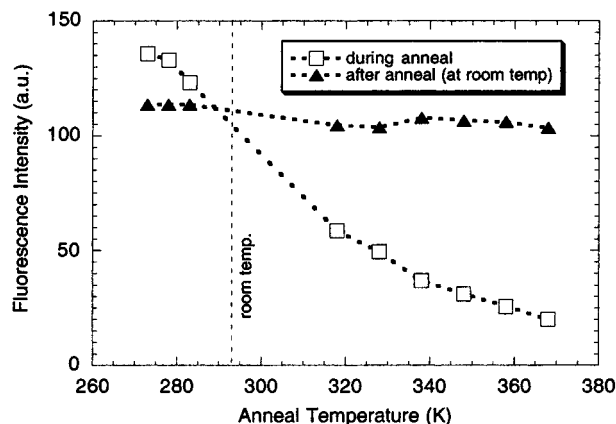


**Figure 7.** Fluorescence emission intensity vs temperature for a sample initially in the red form: open squares, intensity at the annealing temperature; closed triangles, intensity at room temperature after annealing to the indicated temperature. The emission at room temperature is unaffected by the annealing cycles. Increased temperature reduces fluorescence emission, and cooling below room temperature increases fluorescence emission.

## Discussion

**Initial and Final Conversion to the Red Form.** The observed threshold anneal temperatures of  $\sim 320$  K to initiate creation of red poly-PCDA, and 353 K to establish nearly complete conversion to the red form, is similar to previous studies of other poly-PCDA films. Comparisons with these studies are somewhat complicated by the fact that the film properties (e.g., number of layers, use of interlayer divalent ions) and the thermal treatments differ from ours. Deckert et al. studied thermochromism of a 30-layer  $\text{Cd}^{2+}$  salt of poly-PCDA formed by the Langmuir–Blodgett technique on both sides of a hydrophobic glass slide.<sup>23</sup> Absorption spectroscopy was performed as a function of temperature, and similar thermochromic effects were observed, although with some differences that will be discussed below. They observed that changes in the optical absorption spectrum of their poly-PCDA films were fully reversible up to 317 K. Complete conversion to the red form occurred at  $\sim 355$  K, with only a small recovery of the blue form upon returning to room temperature. Mino et al.<sup>22</sup> studied 25-layer  $\text{Ca}^{2+}$  salts of poly-PCDA on quartz and observed full reversibility up to 323 K. After annealing to 343 K, the film was largely converted to the red form, but there was some recovery of the blue form absorption features upon cooling. Absorption spectra were not reported for higher anneal temperatures. Lio et al. studied a trilayer film of poly-PCDA formed on glass substrates modified with a hydrophobic coating<sup>9</sup> and measured absorption spectra at room temperature only, after a series of annealing cycles. They observed very little change in the absorption spectrum at room temperature after annealing to 323 K. The film showed partial conversion to the red form after annealing to 343 K, and complete conversion to red poly-PCDA was observed after annealing to 363 K. The films of Lio et al. were not fully blue to begin with, as absorption features indicated a partial presence of the red form in the film, presumably formed by photochromism during the initial polymerization step. Collectively, these studies, along with ours, indicate that the optical properties of poly-PCDA films can be reversibly altered by heating to approximately 320 K. Overall this change is far less profound than the changes that occur with full conversion to the red form, which occurs at  $\sim 353$  K in our film.

**Intermediate Purple Form.** The purple form appears over the temperature range of 313–343 K, and its appearance at these elevated temperatures is primarily associated with the disappearance of the blue form. Inspection of Figures 4b and 5b show that the purple absorption feature reaches its maximum intensity at about 330 K, while the blue absorption at 640 nm has largely disappeared. However, upon quenching to room temperature the blue form reappears and is still the predominant component of the film. We see no evidence for existence of the purple form at room temperature after any annealing step, as the two-component (red and blue) model provides good fits to all the room-temperature ellipsometry results (Figure 4a). As seen in Figure 4b, the peak of the purple form absorption shifts to shorter wavelength as the temperature increases, and there does not appear to be an isosbestic point associated with the disappearance of blue form and appearance of purple. Since the purple form exists only at elevated temperature, it appears not to be a stable or metastable form of the material, which is interconvertible with the blue form.

These results lead us to propose that the purple form is a thermally distorted configuration of the blue form exhibiting a substantial shift of the absorption spectrum to shorter wavelengths. The purple form may represent a transition state in the conversion to the red form. However, our results indicate that it is energetically favorable for the purple form to revert to the blue, suggesting that the true transition state lies somewhat higher in energy and further along the reaction coordinate toward the red form. This conclusion is supported by the fact that no reversible behavior is seen in these films once they have been converted to the red form; annealing red films does not result in appearance of the purple form or conversion back to the blue form. This conclusion is also consistent with the aforementioned study of Mino et al.,<sup>22</sup> which involved 25-layer samples of  $\text{Ca}^{2+}$  salts of poly-PCDA. They obtained UV–visible absorption spectra, differential scanning calorimeter (DSC) curves, and IR spectra as a function of temperature. The IR spectra support the hypothesis that at elevated temperatures ( $\sim 323$ – $346$  K), a thermally distorted blue form is present. Specifically, it was found that IR absorption bands corresponding to the side chains ( $\text{CH}_2$  scissoring, and  $(\text{CH}_2)_n$  twisting and wagging vibrations) became significantly weaker above 323 K due to disordering. In addition, the film exhibited a melting transition at 346 K as observed with DSC. As mentioned above, nearly complete conversion to the red form for our film did not occur until annealing at 353 K. Therefore, we can expect the hydrocarbon side chains to exhibit significant disordering in the temperature range  $\sim 323$ – $350$  K, while the red form has not yet been fully formed thermochromically. This may account for the purple form we observe.

We see no evidence that the three layers within the film change to the red form at different rates. If this were the case, the multicomponent EMA model would not show good agreement with our results; layers with different optical properties can be distinguished using this model. To completely rule out such an effect, future experiments using a monolayer sample are planned, as we have recently succeeded in producing high-quality monolayer PDA samples.<sup>21</sup>

**Reaction Scheme.** Deckert et al., in a study of thicker  $\text{Cd}^{2+}$  salt films of 5,7-diacetylenes,<sup>24</sup> have proposed a two reaction scheme from blue (B) to red (R) occurring in series, involving a reversible transition to an intermediate

purple (P) form:



In that work, the two-reaction scheme provided a consistent model for absorption spectra obtained over the temperature range of 290–360 K. However, a different reaction scheme was proposed by Deckert et al. in an earlier study of 10,12-diacetylene films including PCDA.<sup>23</sup> The data from that study favored a reversible transition between blue and red forms and an irreversible transition from the purple to red form:



We have carried out first-order kinetic simulations to test whether either of the above schemes is consistent with our results. For any reasonable barriers for the  $B \leftrightarrow P$  reactions, the series kinetic scheme in eq 3 would predict incomplete conversion of  $B \rightarrow P$  upon heating and incomplete reversion of  $P \rightarrow B$  after quenching. This is not consistent with our results, as we observe a complete and reversible transition from the blue form to the intermediate purple form upon heating. As well, there is apparently no energetic barrier to reversion of  $P \rightarrow B$  since the blue absorption features fully recover upon quenching to room temperature. The parallel reaction scheme of eq 4 requires a significant initial presence of the purple form in the film and would predict significant reversibility between blue and red forms at elevated temperatures. Our data are not consistent with these conditions. Thus, according to our kinetic simulations, no kinetic scheme involving a stable or metastable purple form of the poly-PCDA is consistent with our data.

Rather, our data support a mechanism in which the purple form is in fact thermally distorted blue material, involving a substantial shift in the absorption spectrum, as opposed to a significant structural transition that would involve energetic barriers between blue and purple forms. In addition to the observed reversibility between blue and purple forms, we also observe total, irreversible conversion to the red form after heating to 353 K or higher. This is convincingly supported both by the absorption spectra from ellipsometry measurements and from the fluorescence emission experiments. We propose a simple, first-order, irreversible transition from blue/purple to red ( $B \rightarrow R$ ) for this film.

**Kinetic Analysis from Time-Resolved Fluorescence Emission.** The fluorescence intensity measurements confirm that only the red form of poly-PCDA displays strong fluorescence. This is a general property of PDA materials, be they thin films,<sup>6,7</sup> bulk samples,<sup>35,36</sup> or solutions.<sup>37</sup> The blue form does not fluoresce due to the presence of low-lying excited states having the same  $A_g$  symmetry as the ground state.<sup>38</sup> This study establishes that the intermediate purple form is nonfluorescent. Therefore, fluorescence emission is a sensitive gauge of the transition to the red form.<sup>7</sup>

We can then obtain kinetic information for the irreversible transition to the red form by examining time-

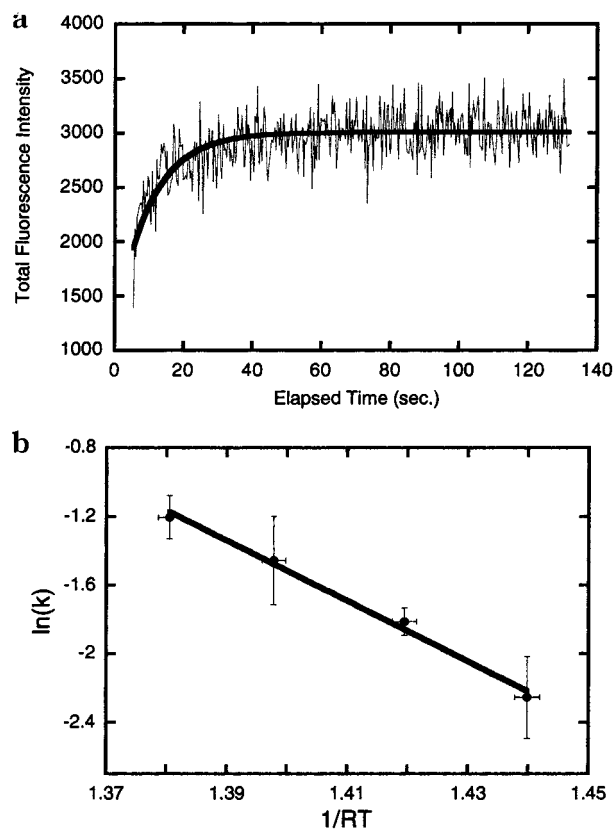


**Figure 8.** (a) Plot of fluorescence vs time at 350 K (circles) with a least-squares fit of eq 7 (solid line). Each data point represents integrated fluorescence intensity between 585 and 720 nm. The fluorescence spectra are acquired every 250 ms with approximately 50 ms delay between each acquisition. The fit provides a value of  $k$  for each measurement. Several fits to each set of data were performed due to uncertainty in the starting time of the measurement. (b) Arrhenius plot [ $\ln(k)$  vs  $1/RT$ ] of several measurements of fluorescence vs time such as in part a. Measurements of  $k$  were acquired at four temperatures (345, 350, 355, and 360 K). The error bars represent the statistical spread of fits at the same temperature. The linear behavior confirms that first-order kinetics provides an accurate description of this system. The energy barrier determined from this plot is  $E = 17.6 \pm 1.1$  kcal mol<sup>-1</sup>.

resolved measurements of fluorescence emission. Assuming first-order kinetics at fixed temperature, the amount of blue poly-PCDA [B] is determined by

$$d[B]/dt = -k[B] \quad (5)$$

Thus

$$[B]/[B_0] = e^{-kt} \quad (6)$$

where  $[B_0]$  is the initial amount of blue and  $k$  is the rate constant. Since only blue and red forms are present, the rate of creation of red poly-PCDA [R] is

$$\frac{[R]}{[R_{\max}]} = 1 - \frac{[B]}{[B_0]} = 1 - e^{-kt} \quad (7)$$

where  $[R_{\max}]$  is the final amount of red poly-PCDA. We assume that the isothermal fluorescence intensity is proportional to [R]. Figure 8a shows a typical plot of fluorescence intensity vs time, in this case at 350 K, with a least-squares fit of eq 7. Along with fitting the rate constant and  $[R_{\max}]$ , we must also account for an offset of the time axis since the sample heating begins after the

(35) Yasuda, A.; Yoshizawa, M.; Kobayashi, T. *Chem. Phys. Lett.* **1993**, *209*, 281–6.

(36) Baughman, R. H.; Chance, R. R. *J. Polym. Sci., Polym. Chem. Ed.* **1976**, *14*, 2037.

(37) Bhattacharjee, H. R.; Preziosi, A. F.; Patel, G. N. *J. Chem. Phys.* **1980**, *73*, 1478–80.

(38) Lawrence, B.; Torruellas, W. E.; Cha, M.; Sundheimer, M. L.; Stegeman, G. I.; Meth, J.; Etamad, S.; Baker, G. *Phys. Rev. Lett.* **1994**, *73*, 597–600.

**Table 1. Comparisons of activation barriers for various PDA films**

ref	monomer	proposed reaction	barrier (kcal mol <sup>-1</sup> )
Two Reaction Scheme, First Step <sup>a</sup>			
24	DCDA, <sup>b</sup> CH <sub>3</sub> (CH <sub>2</sub> ) <sub>11</sub> C≡CC=C(CH <sub>2</sub> ) <sub>3</sub> COOH <sup>c</sup>	B → P	21.7 <sup>d</sup>
24	TTCDA, <sup>e</sup> CH <sub>3</sub> (CH <sub>2</sub> ) <sub>15</sub> C≡CC=C(CH <sub>2</sub> ) <sub>3</sub> COOH <sup>c</sup>	B → P	21 <sup>d</sup>
23	TCDA, <sup>f</sup> CH <sub>3</sub> (CH <sub>2</sub> ) <sub>9</sub> C≡CC=C(CH <sub>2</sub> ) <sub>8</sub> COOH <sup>c</sup>	B → R <sup>g</sup>	22.5
23	PCDA, CH <sub>3</sub> (CH <sub>2</sub> ) <sub>11</sub> C≡CC=C(CH <sub>2</sub> ) <sub>8</sub> COOH <sup>c</sup>	B → R <sup>g</sup>	21.5
Two Reaction Scheme, Second Step			
23	TCDA <sup>c</sup>	P → R	23
23	PCDA <sup>c</sup>	P → R	22.5
Single Reaction Scheme			
this work	PCDA <sup>h</sup>	B → R	17.6 ± 1.1

<sup>a</sup> This step is considered to be reversible in the reaction schemes considered. <sup>b</sup> 5,7-Docosadiynoic acid. <sup>c</sup> Film consisted of Cd<sup>2+</sup> salts of the particular PDA molecule, with 30 layers on both sides of a hydrophobic glass slide. Polymerization was performed after the monomer film was transferred to the glass slide. <sup>d</sup> Barrier is for a "high density" film of molecular area 22 Å<sup>2</sup> molecule<sup>-1</sup>, comparable to our films. "Low density" films (26 Å<sup>2</sup>/molecule) exhibited slightly higher activation barriers.<sup>24</sup> <sup>e</sup> 5,7-Tetracosadiynoic acid. <sup>f</sup> 10,12-Tricosadiynoic acid. <sup>g</sup> Deckert et al. suggest that a reversible reaction step between blue and purple forms (B → P) may occur as well.<sup>24</sup> <sup>h</sup> This work. Films in this study were pure PCDA monomers, polymerized on the Langmuir trough as a trilayer and then transferred to hydrophilic Si substrates.

data acquisition has started. Before the sample is in place, a large amount of excitation light is scattered from the stage into the collection fiber. Once the sample is placed on the stage, the scattered light is greatly reduced, allowing us to determine the offset of the time axis to within two spectral acquisition windows (±500 ms). This uncertainty is taken into account in determining the rate constant from the fit. The rate constant at a fixed temperature  $T$  is given by

$$k = Ae^{-E/RT} \quad (8)$$

where  $E$  is the energy barrier,  $R = 1.9 \times 10^{-3}$  kcal mol<sup>-1</sup> K<sup>-1</sup>, and  $A$  is the pre-exponential factor. Therefore, the slope of an Arrhenius plot [ $\ln(k)$  vs  $1/RT$ ] will be the energy barrier  $E$ . The result is plotted in Figure 8b. The error bars represent the statistical spread of fits at the same temperature. The linear behavior confirms that first-order kinetics provides an accurate description of this system. From the Arrhenius plot we determine  $E = 17.6 \pm 1.1$  kcal mol<sup>-1</sup>. In Table 1 we compared this to activation barriers measured by Deckert et al. for a range of thicker Cd<sup>2+</sup> salt PDA films.<sup>23,24</sup> As discussed previously, Deckert et al.'s models consisted of two different two-reaction schemes both involving a distinct purple form separated by an energy barrier from the blue form; this complicates any direct comparison with our results. Nevertheless, all of the activation barriers from the schemes of Deckert et al. are somewhat larger than the present measurement. The fact that our films are only three layers thick and lack metal ion complexation may affect the kinetics of the transition significantly. In particular, our film is likely to exhibit fewer defects and stronger thermal coupling between and within layers due to their crystallinity and structural registry. These factors would likely tend to reduce the energy barrier. The extremely low substrate roughness and lack of metal salt ions in our film may also enhance the ability of the PDA molecules to undergo structural changes compared with the thick films. This would also tend to reduce the energy barrier. Direct comparisons of different films in the same experiment would be needed to verify these effects.

**Thermal Reduction of Fluorescence Emission.** The decrease in fluorescence emission from red films at elevated temperature is not accompanied by a similar decrease in absorption. Rather, the absorption spectrum of red films remains constant at elevated temperatures, according to ellipsometric measurements. Therefore, the

fluorescence emission must be reduced by a substantial enhancement of nonradiative decay processes, as opposed to changes in the absorption characteristics.

As mentioned above, Mino et al.<sup>22</sup> observed significant thermal fluctuations of the side chains of a blue film when annealed above 323 K. Furthermore, these fluctuations lead to a disordered film structure. Unfortunately, they did not perform thermal cycling experiments; only a single increasing temperature ramp was used. Therefore, their study does not establish the degree of order in the film at room temperature in the red form (i.e., after annealing). Recent evidence suggests that the thermochromic red form is in fact *more* ordered than the blue form at room temperature, at least for trilayer poly-PCDA films. In the study of Lio et al.,<sup>9</sup> the CH<sub>2</sub> antisymmetric stretching band in the IR spectrum at room temperature increased in intensity and downshifted in frequency after annealing a blue film to 343 K and remained so after further annealing up to 383 K. These IR spectral changes indicate a more ordered side chain arrangement after the thermochromic transition.<sup>9</sup> Furthermore, Lio et al. obtained molecular-lattice resolved images of blue and thermochromic red poly-PCDA trilayer films using AFM. The images clearly demonstrated that the side chains are more ordered in the thermochromic red form than the blue. This effect may also be related to our observation that fluorescence emission from the thermochromic red film at room temperature is enhanced by further annealing the film at temperatures up to at least 368 K (Figure 6). The additional anneal may promote ordering of the side chains in the thermochromic red film when cooled back to room temperature. Several factors therefore suggest a general correlation between side chain ordering and fluorescence emission.

The above results indicate that we can expect significant fluctuations of the side chains, and presumably the backbones to which they are attached, at elevated temperatures. Furthermore, these thermally induced molecular fluctuations lead to a reduction of molecular order at elevated temperatures. Both of these factors may enhance nonradiative de-excitation pathways. If so, we would then expect that cooling a photochromic red film would increase the fluorescence emission. This is indeed observed (Figure 7). Further studies of the vibration and emission spectra of these films as a function of temperature are required to investigate this hypothesis more rigorously.



### Summary

We have shown that spectroscopic ellipsometry can be used to monitor thermochromism in ultrathin poly-(diacetylene) films. Spectroscopic ellipsometry reveals that trilayer films of poly-PCDA exhibit a partially reversible transition from the blue form to an intermediate purple form, followed by an irreversible transition to the red form. The purple form appears to be thermally distorted blue material. The purple form is present only at elevated temperatures and exhibits a large, reversible shift in the absorption spectrum to shorter wavelengths. From time-resolved fluorescence experiments we determine an energy barrier of  $17.6 \pm 1.1$  kcal mol<sup>-1</sup> for the irreversible transition from blue/purple to red forms. Only the red form exhibits significant fluorescence emission. Thermal effects reduce fluorescence emission at elevated temperatures. It is likely that thermal fluctuations of the side chains reduce fluorescence emission.

**Acknowledgment.** We gratefully acknowledge M. L. Thomas who implemented the heating stage used for these measurements and M. B. Sinclair and J. A. Hunter who assisted in setting up the time-resolved fluorescence experiments. We gratefully acknowledge N. D. Shinn for providing a thorough review of this manuscript. R. W. C. acknowledges the support of the Natural Sciences and Engineering Research Council of Canada. Sandia is a multiprogram laboratory operated by Sandia Corporation, a Lockheed Martin Company, for the United States Department of Energy under Contract DE-AC04-94AL85000.

### Appendix

**Ellipsometric Analysis. A. Lorentz Oscillator Parameterization.** The complex dielectric function of the poly-PCDA “red”, “blue”, and “purple” forms as a function of photon energy is modeled as a sum of Lorentz oscillators, given by

$$\bar{\epsilon}(E) = \epsilon_1(\infty) + \sum_{i=1}^N \frac{A_i}{(E_{c,i}^2 - E^2 - iB_iE)} \quad (\text{A1})$$

We employ the minimum number of oscillators required to characterize the major absorption features of the data, as well as the baseline absorption. The values of  $\epsilon_1(\infty)$ ,

**Table 2. Lorentz Oscillator Model Parameters for Poly-PCDA Films for the Wavelength Range 450–700 nm**

$i$	$\epsilon_1(\infty)$	$A$ (eV <sup>2</sup> )	$B$ (eV)	$E_c$ (eV)
“red” form				
	3.6958			
1		0.26902	0.05363	2.251
2		0.91248	0.23264	2.4477
3		73.179	1.6481	3.8619
“blue” form				
	1.2455			
1		0.25339	0.093042	1.947
2		3.802	0.76813	2.3277
3		50.508	0.77156	3.5966
“purple” form				
	0.79317			
1		0.21002	0.13649	2.094
2		0.61777	0.20296	2.301
3		2.2458	0.55236	2.529
4		52.152	0.79345	3.5905

amplitude,  $A$ , width,  $B$ , and the peak energy,  $E_c$ , of the the three poly-PCDA forms are given in Table 2. The complex index of refraction is related to the complex dielectric function by

$$\bar{N}^2 = \bar{\epsilon}^2 \quad (\text{A2})$$

**B. Effective Medium Model.** Inhomogeneous films containing two or more distinct components can be successfully modeled using an effective medium approach.<sup>33</sup> In this procedure the optical constants of an “effective film” are constructed from the optical constants of the constituent materials and treated as a single layer in the optical model. In the Bruggeman effective medium approximation used here,<sup>33</sup> the complex index of the effective film,  $N_e$ , is obtained from

$$\sum_i f_i \frac{\bar{N}_i^2 - \bar{N}_e^2}{\bar{N}_i^2 + \bar{N}_e^2} \quad (\text{A3})$$

where  $N_i$  and  $f_i$  are the complex indices of refraction and volume fractions of the constituent materials.  $N_i$  for the poly-PCDA forms are as given in Section A, and  $f_i$  are the adjustable parameters in the model.

All ellipsometric models and calculations are included in the standard analysis software provided with the spectroscopic ellipsometer (J. A. Woollam Co., Lincoln, NE).

LA991580K